ANNALS OF GEOPHYSICS, VOL. 47, N. 5, October 2004

Results from the temporary installation of a small aperture seismic array in the Central Apennines and its merits for local event detection and location capabilities

Thomas Braun ([1]), **Johannes Schweitzer** ([2]), **Riccardo M. Azzara** ([1]), **Davide Piccinini** ([1]), **Massimo Cocco** ([3]) **and Enzo Boschi** ([3])

([1]) *Istituto Nazionale di Geofisica e Vulcanologia, Osservatorio Sismologico, Arezzo, Italy*

([2]) *NORSAR, Kjeller, Norway*

([3]) *Istituto Nazionale di Geofisica e Vulcanologia, Roma, Italy*

Abstract

In order to evaluate the detection and localisation improvement of a small aperture array in the Northern Apennines, we installed an irregularly spaced test configuration in the vicinity of Città di Castello (CDC) for a period of two weeks. The experimental array consisted of nine 3-component stations with inter-station distances between 150 m and 2200 m. Seismic data were digitised at 125 Hz and telemetered to a mobile acquisition, processing and storage centre. The data could only be recorded in trigger mode. The peculiarity of the test array installation was the exclusive use of 3-component sensors at all array sites, which also allowed beamforming for *S*-phases on the horizontal components. Since the altitudes of the single array sites differed considerably among each other, for *f-k* analysis and beamforming an elevation correction was included. During the two weeks of operation about 20 local earthquakes with magnitudes M_L<2.6, 1 regional, and several teleseismic events were recorded. In addition to these events, the array occasionally triggered on coherent noise-signals generated by local industrial activity. The data analysis was performed by means of *f-k* analysis and beamforming, providing wavenumber characteristics of the incident plane wave. Typical apparent velocities were determined to be 4.8 km/s and 6 km/s for *Pg*-phases and ~10 km/s for *Pn*-phases. We observed local seismic events, which occurred just beneath the array. In these cases wavefronts with unusual high apparent velocities, similar to those found for the *Pn*-phase, were observed. Since no continuously recorded array data were available, we extrapolated the lower detection magnitude threshold as a result of the *SNR* improvement due to array beamforming. Compared to the actual detection threshold of M_T~1.6 reached by the national seismic network in this area, a nine element array would improve this value up to M_T~0.8.

Key words *seismic array – beamforming* – f-k *analysis – Central Apennines – Città di Castello*

1. Introduction

The National Earthquake Survey Centre (CNT) of the Istituto Nazionale di Geofisica e Vulcanologia at Rome manages the seismic surveillance of Italy. The national real-time monitoring system consists of two seismic networks, operating on different scales:

i) RSNC – the national seismic network – has more than 100 short-period stations. Data

Mailing address: Dr. Thomas Braun, Istituto Nazionale di Geofisica e Vulcanologia, Osservatorio Sismologico, Via U. della Faggiuola 3, 52100 Arezzo, Italy; e-mail: braun@ingv.it

are transmitted via dedicated telephone lines to the processing centre at the INGV-Rome. The detection magnitude threshold M_T^{RNSC} varies between $1.5<M_W<2.6$, depending on the spatial station density in the respective area (Cattaneo *et al.*, 2002).

ii) MedNet operates 7 seismic broadband stations in Italy, and data are used by the CNT to perform local magnitude estimates and Centroid Moment Tensor solutions.

High-resolution seismicity studies, as recently realised in the Central Apennines with a dense seismic wide-band network (Piccinini *et al.*, 2003), revealed strong and formerly unknown background seismicity with magnitudes distinctly below M_T^{RNSC}. About 2200 seismic events ($M_L<3.2$) were reported within a 6 month period, most of them confined in the upper crust. Due to the lower spatial density, the RSNC-bulletin reports, for the same period and area, only about the strongest 10% of this instrumental seismicity. Experiences from Scandinavia and Germany also show that seismic arrays can dramatically improve the monitoring threshold and make an important contribution to seismic monitoring (*e.g.,* Mykkeltveit and Bungum, 1984; Kværna, 1989; Harjes, 1990).

Our interest in a seismic array in Central Italy arises from the need to improve the present low spatial density of the seismic network, especially in Tuscany, with a centralised array installation. A small aperture array, located near

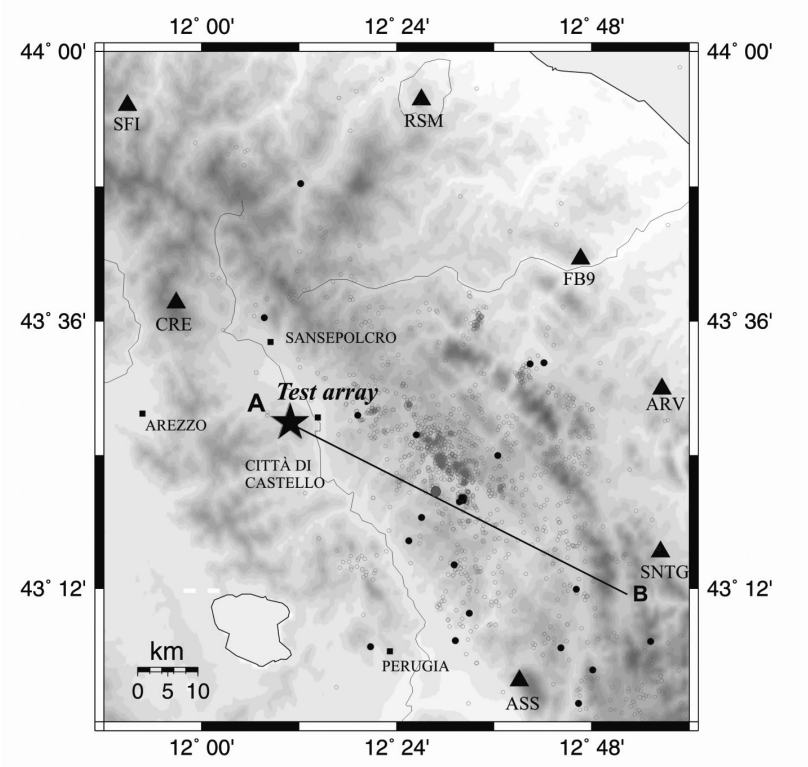

Fig. 1. Location of the test array site near Città di Castello (asterisk). Triangles indicate the locations of the RSNC-stations during the CDC-array experiment. The epicentres of the local seismic events recorded during the array experiment are plotted with black dots; the grey dots represent the background seismicity as recorded during the following month by a dense local seismic network (2nd field experiment). The line A-B indicates the direction of the section shown in fig. 7.

the Apennines, could distinctly lower the detection threshold for the above mentioned background seismicity and improve the seismic monitoring system.

Since no permanent seismic array is currently operating in Italy, we realised a temporary small aperture seismic array installation in the Upper Tiber Valley (asterisk in fig. 1), in the vicinity of Città di Castello (CDC). The purpose of the two-week long experiment was to study the merits of a seismic array for local event detection and location capabilities by applying classical *f-k* analysis techniques as described, *e.g.,* by Kværna and Dornboos (1986).

The main scientific objectives of the present paper are:

1) *P*- and *S*-wave beamforming and *f-k* analysis for local and regional events observed by this test array.

2) Phase discrimination and association of detected signals to seismic events.

3) Study of the wave-number characteristics of signals and noise at this array site.

2. Configuration of the test array

Conventional small aperture array installations like, *e.g.,* ARCES, FINES, GERES, or NORES are equipped primarily with vertical sensors. The innovative aspect of the test array installation described in the presented study is the exclusive usage of 3-component sensors at all array sites. This also allows *S*-wave beamforming on the horizontal components.

2.1. *Instrumentation*

Important prerequisites for the realisation of a seismic array are uniform instrumentation, centralised timing and continuous recording. INGV's Task Force has a Mobile Acquisition Centre (MAC) with one mono-component and nine 3-component seismic stations at its disposal, to be employed in the case of a seismic emergency. The MAC is able to manage simultaneously the real time acquisition of 28 channels, also fulfilling the condition of a centralised timing (GPS) and was therefore an appropriate instrument for this array experiment. The only limitations of the MAC are given by its internal memory capabilities, which do not allow continuous data acquisition for more than approximately 5 min. Therefore, every single field station runs in a local trigger mode (STA/LTA) and offers once triggered data to the MAC. The centralised acquisition starts only if the pre-set number of coincidence triggers is reached or exceeded. The MAC's instrumentation pool consisted of nine seismic 3-component stations, equipped with Lennartz 5800 digitisers (12 bit gain ranging, sampling rate 125 sps*)* and LE 3D-5 s seismometers.

2.2. *Choice of array site*

The choice of an appropriate logistics base for the MAC had to fulfil several requirements. Besides the necessity to keep the largest possible distance from civilisation, a panoramic site had to be chosen to guarantee the proper work of the digital telemetry. This point was not only crucial for the test array installation itself, but also for the successive deployment of a local network in the Central Apennines (up to 40 km from the MAC), in the framework of a second 6 month long field experiment (Cocco, 2001). The final choice to install the array in a hilly zone about 5 km W of Città di Castello represented a compromise between the requirements of the two seismic field experiments in array and network configuration. However, a better site for a seismic array should be if possible further away from civilisation (*i.e.* man-made noise sources), with less topography inside the array area.

2.3. *Array geometry*

In order to guarantee azimuth independent receiver characteristics, small aperture arrays, like the ones installed in Norway (ARCES, NORES, SPITS), Finland (FINES), or Germany (GERES), have an approximately circular configuration. The radii of the concentric circles and the position of the respective stations were determined by correlation analysis of noise and signal samples recorded at the array sites, and

were additionally chosen in such a way, that the inter-station distances allow an optimal spatial sampling of the signal wavefield.

The purpose of a test array installation is to determine the wavefield characteristics by calculating the respective correlation coefficients for signal and noise. Therefore, the test array has to be configured with a rather irregular geometry, to obtain as many different inter-sensor distances as possible (Schweitzer *et al.*, 2002). The purpose of such a site survey is to become acquainted with the wave-number characteristics of signals and noise, which is necessary to design an array configuration that optimises noise suppression, while preserving the signal.

Figure 2 shows the configuration of the test array, as it operated for two weeks near CDC. The respective station-to-station distances range from 150 to 2200 m. However, the array's slight extension in N-S direction results in a slightly better azimuthal resolution for the tectonically active area east of CDC (Central Apennines). The array transfer function (ARF) of the CDC test array is illustrated in fig. 3. The

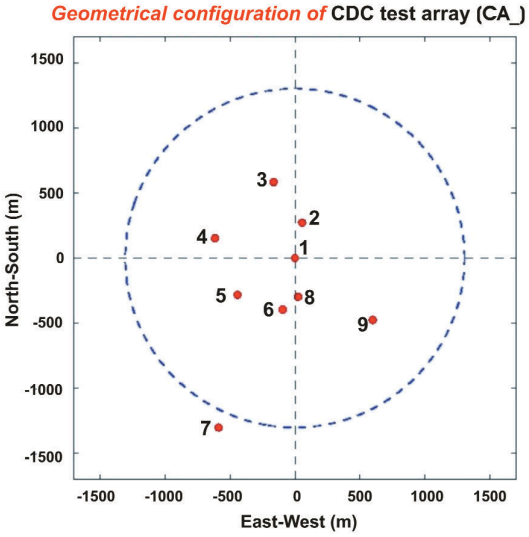

Fig. 2. Geometrical configuration of the 9-component test array, temporarily installed near CDC.

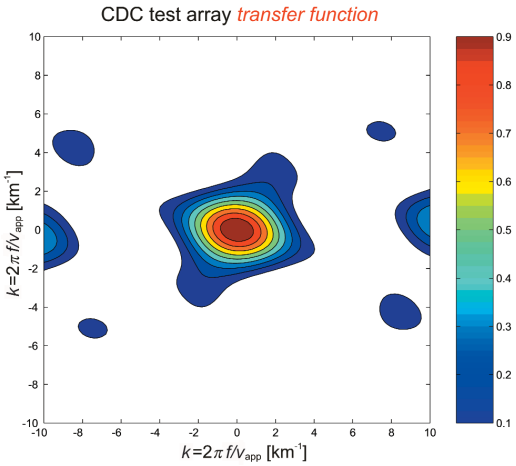

Fig. 3. Array response function of the CDC test array of fig. 2.

rainbow colour palette indicates the relative power of the ARF below its maximum.

Compared to the small scale arrays mentioned above, the CDC-array's aperture of $a=2$ km is something in between the 9-elements array of SPITS ($a=1$ km) and the 25-elements array of GERES ($a=4$ km). The 16-elements FINES array has about the same aperture of $a=$ $=2$ km. Since for long wavelengths ($\lambda \gg a$) an array responds like a single station, the analysis range of small aperture arrays like the CDC-array is aimed for signals of local and regional seismic events. The array's small aperture causes a relatively wide main lobe of the ARF, which makes it impossible to distinguish the planewave characteristics backazimuth and apparent velocity, for seismic signals with small wavenumber differences. Despite its irregular configuration, the azimuthal resolution of the CDC-array is acceptable.

2.4. *Set of available data*

During the two weeks field experiment (October 10-24, 2000), we ran the MAC with a coincidence trigger of 4. In this way, we recorded 20 local ($1.0<M_L<2.6$), 1 regional, and several

teleseismic events and 2 sonic booms. Furthermore, the array occasionally triggered on coherent 3 Hz-noise signals, which may have been generated by industrial activities.

Besides these observations, we recorded a set of noise windows lasting several minutes to analyse the noise correlation throughout the array. These noise samples were collected three times daily, for the entire period of the array installation in order to obtain a statistical significant data set (Braun and Schweitzer, 2002). Nevertheless, correlation analysis and the determination of the array gain go beyond the scope of the present report and will be subject of a special paper.

3. Station elevation correction

The purpose of *f-k* analysis is to determine the backazimuth and the apparent velocity of the incident planewave front of a selected phase. The process of beamforming consists in summing up the seismic traces after relative time shifting with respect to the delay times, which result from the wavenumber analysis of the studied seismic phase and the array geometry. In this way, the incoherent noise is suppressed and only the coherent signals interfere constructively. Overviews on the principles of array beamforming can be found, *e.g.,* in Harjes and Henger (1973) or in Schweitzer *et al.* (2002).

For the case where the single array sites are located in the same horizontal plane, the time delay for a plane wave can be calculated at each site *j*,with respect to a reference site, as follows:

$$\tau_j^{\text{hor}} = \frac{d_j}{v_A} = \frac{-x_j \cdot \sin\Phi - y_j \cdot \cos\Phi}{v_A} \qquad (3.1)$$

(d_j=horizontal distance; v_A=apparent velocity; (x,y)=horizontal coordinates; Φ=backazimuth).

Since the altitude differences between the single sites z_j of the CDC test array were in the range of the inter-station distances, an elevation correction had to be applied (for details see Schweitzer *et al.*, 2002).

In this case eq. (3.1) has to be adjusted by an additional term

$$\tau_j^{\text{ver}} = \frac{z_j \cdot \cos i}{v_c} \qquad (3.2)$$

and hence the time delay for each site *j* becomes

$$\tau_j = \tau_j^{\text{hor}} + \tau_j^{\text{ver}} = \frac{-x_j \cdot \sin\Phi - y_j \cdot \cos\Phi}{v_A} + \frac{z_j \cdot \cos i}{v_c} \qquad (3.3)$$

(v_c=mean velocity of the *P*- or *S*-wave beneath the array in the uppermost crust; i=incidence angle; z_j=relative elevation difference).

Now, the time delay τ_j is also influenced by the local crustal velocity v_c, which is to be set according to the seismic-phase type (*P* or *S*) on which beamforming or *f-k* analysis is performed.

In order to find the «best» mean velocities for the elevation correction, we performed *f-k* analysis for some test events, using v_c-values in a range from 1-10 km/s. The maximal beam power was found when using $v_c^P = 4.5$ km/s for *P*-phases and $v_c^S = 2.5$ km/s for *S*-phases.

A station elevation correction must be considered if the time shift caused by the altitude differences amounts to approximately 1/2 of the time delay between two samples. The CDC array data have a time delay of 8 ms, *i.e.* we have to apply the elevation correction if the time delays become about 4 ms or larger. Assuming a *P*-wave (*i.e.* $v_c^P = 4.5$ km/s) approaching the array directly from below, an elevation differences of *ca*. 20 m will already result in a time delay of more than 4 ms.

4. Examples for *f-k* analysis and array beamforming

In this section, we show some representative examples for *f-k* analysis and beamforming with seismic data recorded by the CDC-array. Keeping in mind a possible future small aperture array installation in Central Italy, we present the wavenumber characteristics of local and regional seismic events and emphasize on special conditions to be considered, like the observation of seismic events, which occur just beneath the array.

The array data were processed using the broadband *f-k* algorithm of Kværna and Dorn-

boos (1986), which represents an extension of the original single frequency wavenumber analysis of Capon (1969). To study systematically location errors of a small aperture array, a long time series of data must be available. Only then systematic effects of lateral heterogeneities beneath the array on the parameters of the wavefront propagation can be statistically investigated. Deviations of the observed planewave parameters azimuth and apparent velocity from theoretical predictions are well known and were studied for many arrays (see *e.g.,* Schweitzer, 2001b). However, when enough events from different backazimuths and distances have been observed, the measured slowness vectors can be corrected for these systematic effects and then the remaining uncertainty of an (automatic) *f-k* analysis of small aperture array data will be between 1 and 2 s/deg, depending on the aperture of the array. With this uncertainty an automatic identification of local or regional phases (*P*, *Pn*, *Pg*, *Sn*, *Sg*, or *Rg*) will be possible with a backazimuth error of only some degrees. Therefore, in the case of a permanent array installation, the calibration of the array is one of the most important issues during the first years of data recording.

One aspect of the experimental array installation was the use of the horizontal components for *S*-wave detection and *f-k* analysis, possible because the CDC-test array was equipped at all sites with 3-component seismometers. Thereby, the *S*-phase could be analysed on these components on which it has its highest *SNR*.

4.1. P-*wave beamforming*

The single steps for the performed slowness analysis of the *P*-phase were:

i) bandpass filtering of the traces, according to *SNR* and main frequency content of the signal;

ii) *f-k* analysis with application of the discussed correction due to the topography;

iii) beamforming by delay-and-sum of the traces with respect to the *f-k* results.

In a first step, we applied the analysis (i-iii) to a local seismic event (fig. 4), located by RSNC in the Central Apennines at about 40 km ESE of the CDC-array (M_L=1.8). The *f-k* analy-

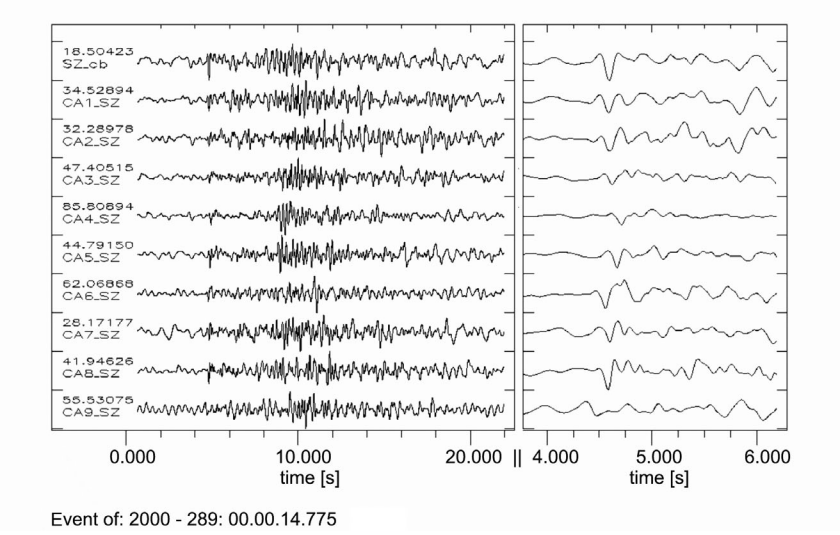

Fig. 4. Vertical seismograms (CA1_SZ-CA9_SZ) and corresponding beam (upper trace SZ_cb), calculated for apparent velocity and backazimuth, determined by the *f-k* analysis of fig. 5. The right side shows a blow-up for the *Pg*-phase.

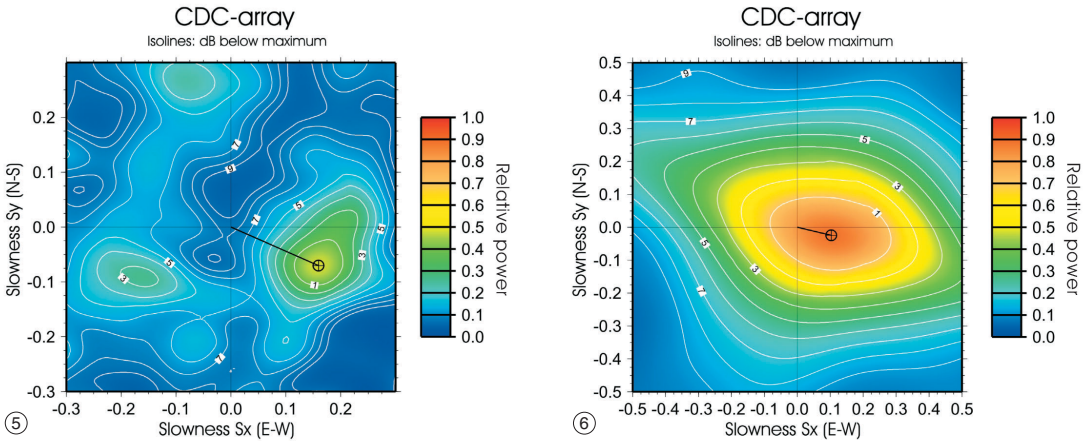

Fig. 5. *F-k* analysis based on the nine bandpass filtered (2.0-6.0 Hz) vertical traces of a local seismic event (M_L=1.8) occurred at 40 km ESE from the CDC-array. The maximum peak level (relative power 0.48) is found for v_{app}=5.74 km/s and backazimuth = 113.7°).

Fig. 6. *F-k* analysis of the nine bandpass filtered (0.8-2.5 Hz) vertical records of a regional seismic event (M_L= =3.5), located in the Greece-Albania border region. For the maximum peak level (relative power=0.88) an apparent velocity of v_{app}=9.43 km/s was determined, reaching the array from a backazimuth of 103.3°.

sis reveals maximum power for the *Pg*-phase at a backazimuth of ~114° and an apparent velocity of v_A=5.74 km/s (fig. 5).

The lower nine seismic traces (CA1_SZ-CA9_SZ) in fig. 4 show the vertical components and the upper trace (SZ_cb) represents the beam according to the former wavenumber analysis (fig. 5). The right side of fig. 4 shows a respective blow up around the *Pg*-phase. Noticeably the *Pg* onset is much clearer and the coda is suppressed. The *SNR*-enhancement of the beam compared to the bandpass filtered traces (2-6 Hz) is evident. The secondary maxima in fig. 5 are not due to sidelobes of the array transfer function (see fig. 3) but caused by disturbing coherent seismic energy, simultaneously reaching the array.

Detailed *f-k* analyses of *Pg* onsets from other local events, at epicentral distances between 40 and 150 km, showed apparent velocities of $4.8 < v_A^{Pg} < 6$ km/s, whereas the *Pn* velocities are clearly characterised by higher values, as expected.

Figure 6 shows the result of the *f-k* analysis for a *Pn*-phase of a regional seismic event of M_L=3.5, located at the Greece-Albania border region (NEIC). With respect to the CDC-array the epicentre lies at a distance of 775 km with a backazimuth of 118°. The theoretical ray parameter for this *Pn*-phase is 13.37 s/deg, corresponding to an apparent velocity of 8.31 km/s. The *f-k* analysis performed in the passband of 0.8-2.5 Hz reveals for the maximum coherent signal energy an apparent velocity of v_A^{Pn}=9.43 km/s at a backazimuth of 103.3°. The relative power for this *f-k* estimate of 0.88 indicates high coherence of the signal and thereby a reliable analysis result.

Given only this observation, we can only speculate on the causes of such unusual high apparent velocity and the ~15° deviation from the theoretical backazimuth. Possible candidates could be the presence of abnormal velocities beneath the array in the crust or in the uppermost mantle, or dipping layers in the crust or of the Moho itself, demonstrating the need for an array calibration.

We find unexpectedly high *Pg* velocities for events with a hypocenter directly beneath the array. In this case the incidence angle of the in-

coming wavefront becomes much steeper than for a *Pg*-wave at larger distances. In principle, the measured apparent velocity can reach a near infinite value. In this case a correct phase identification based on the apparent velocity is not possible. As an example, we show data from a local seismic event, located 27 km east from the array at a depth of 24 km (gray dots in figs. 1 and 7).

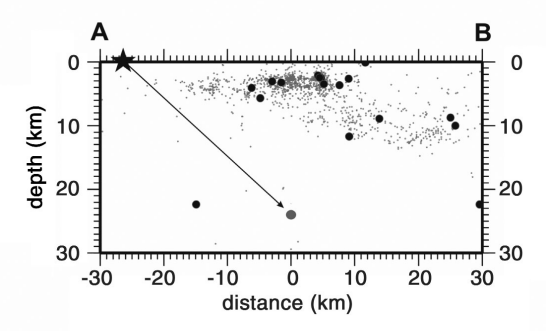

Fig. 7. WNW-ESE section (A-B) of the seismicity plotted in fig. 1. The emphasized local seismic event (M_L=2.5) occurred beneath the CDC-array at 27 km E from MAC at a depth of 24 km.

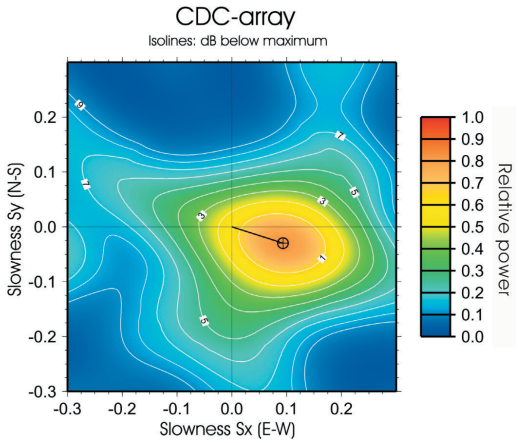

Fig. 8. *F-k* analysis based on the nine bandpass filtered (2.0-4.0 Hz) vertical seismograms of the local seismic event plotted in fig. 7. Maximum energy (relative power=0.86) is found for an apparent velocity of 10.0 km/s in a backazimuth of 107.4°.

The hypocenter was localised by using the onset times at the RSNC stations and from one of the array sites. Figure 7 shows seismicity as plotted in fig. 1, on a vertical section along the line A-B.

As illustrated in fig. 8, the *f-k* analysis for the bandpass filtered (2-4 Hz) vertical recordings of the *P*-wave reveals a peak for the apparent velocity of v_A^{Ps}=10.0 km/s and a backazimuth of 107.4° with a relative power of 0.86. For a typical *Pg*-phase this apparent velocity measure is far too high and rather typical for a *Pn*-phase. This indicates that the wavefront as a direct wave impinges under a very small incidence angle of approximately 45°, and thus confirms the location of the hypocentre just beneath the array.

The seismic traces of this event recorded by the CDC-array are illustrated in fig. 9. The *P*-wave beam (upper trace) calculated after delaying the recordings of the vertical components according to the result of the *f-k* analysis, showed a clear improvement of the signal noise ratio and the *P*-wave coda (*e.g.,* trace CA4_SZ in fig. 9) was suppressed significantly. As mentioned above, for direct waves generated by seismic events, occurring just beneath the array, almost any apparent velocity value can be expected. Automatic event detection processing algorithms running at the formerly cited arrays are tuned for seismic events in distances greater than 100 km.

A triggering algorithm operating at a future permanent array installation in Tuscany should also be able to detect local seismicity. Parameters for such algorithms would have to be tuned to the wavenumber characteristics of these very local seismic events. This could be achieved by considering the *S-P* travel-time difference measured on the corresponding beams and integrating the array-analysis result (onset time, backazimuth and apparent velocity of the *P* and *S* onsets) into the local network localisation routine. Modern location routines as, *e.g.,* HYPOSAT can easily handle such different parameter types in one common inversion (Schweitzer, 2001a).

4.2. S-*wave beamforming*

Array processing of *S*-waves can also be performed using conventional seismic arrays which

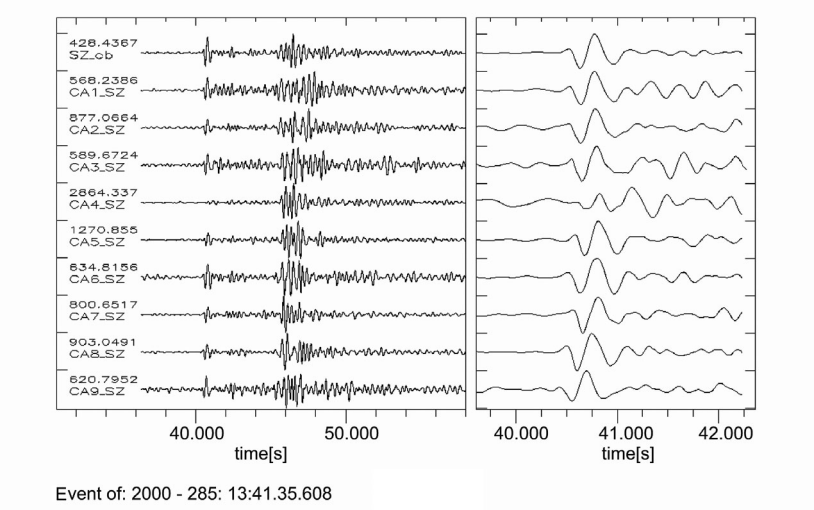

Fig. 9. Vertical seismograms (CA1_SZ-CA9_SZ) and corresponding beam (upper trace SZ_cb), calculated for the apparent velocity and backazimuth, determined by the *f-k* analysis of fig. 8. The right side shows a blow-up of the *Pg*-phase.

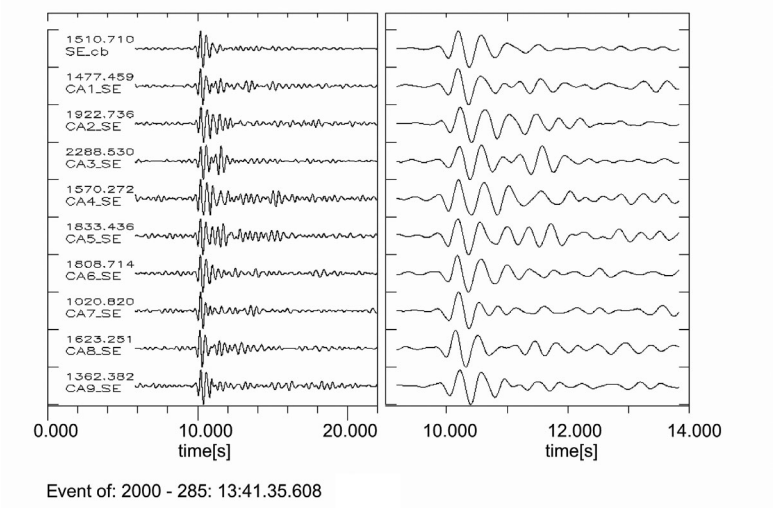

Fig. 10. The E-W component records (CA1_SE-CA9_SE) of the seismic event from fig. 7. The upper trace shows the *S*-beam calculated for the *Sg*-phase, after delaying the traces according to the apparent velocity and the backazimuth determined by the *f-k* analysis from fig. 11a. The right side shows a blow-up of the *Sg*-phase.

are mainly composed of vertical sensors (as, *e.g.,* NORES or FINES). However, it is well known that the ground movement due to *S*-waves can be observed much better on horizontal than on vertical components. Given the restrictions due to data transmission and storage capabilities and last but not least the budget limits, an array should be built, which records all three compo-

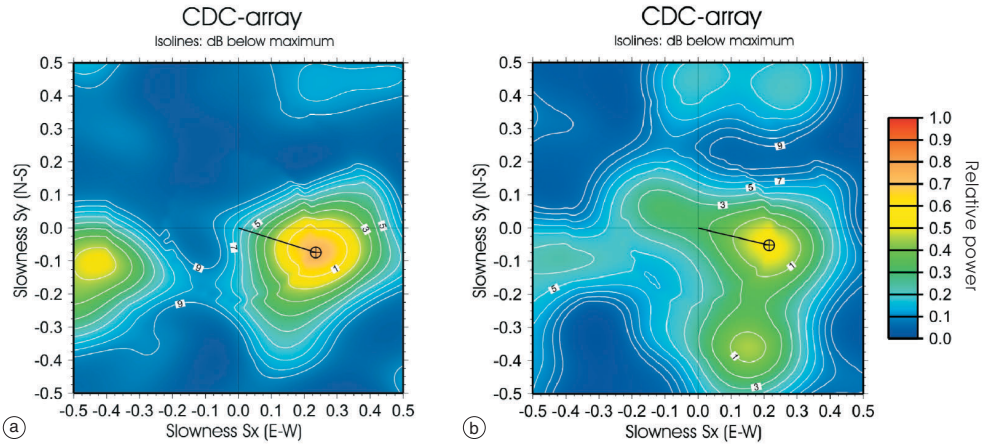

Fig. 11a,b. a) *F-k* analysis performed on the E-W records of the *S*-phase. The maximum peak corresponds with an apparent velocity of v_{app}=4.05 km/s and a backazimuth of 107.5° (relative power=0.74); b) *f-k* analysis performed on the N-S records of the *S*-phase. The maximum peak level (relative power=0.52) is found for an apparent velocity v_{app}=4.52 km/s, reaching the array from a backazimuth of 103.5°.

nents of ground motion. Fortunately, in the case of the CDC-array, we installed a 3-component seismometer at each of the nine array sites. This allowed the application of all the array techniques to horizontal components for the processing of *S* type onsets.

To demonstrate this application, we analysed the *Sg*-phase from the same local event shown and discussed in figs. 7 to 9. Figure 10 illustrates the seismograms from the E-W components (CA1_SE-CA9_SE). The upper trace shows once again the beam, now calculated for the *Sg*-phase. Note the distinct *SNR*-improvement in the *S*-beam, in which all non-coherent signals, like *S*-coda and the whole *P*-phase energy are suppressed successfully. Figure 11a shows the result of the *f-k* analysis for the *Sg*-phase as recorded on the E-W components, used to calculate the beam trace in fig. 10. The results of the *f-k* analysis are an apparent velocity of v_A^{Sg}=4.05 km/s, a backazimuth of 107.5°, and a relative beam power of 0.74. The backazimuth fits very well with the result for the *Pg* onset and again the observed apparent velocity is too high for a normal *Sg* onset but agrees well with an event location beneath the array. As for the *P*-wave analyses, the secondary maxima are not due to sidelobes of the array-transfer function (see fig. 3) but caused by other coherent seismic energy.

The recording quality of the *S*-wave on the N-S components is still inferior, as shown by the results of the *f-k* analysis (fig. 11b). The relative power reaches a lower value of 0.52, which indicates less coherent energy on these components, however, the *f-k* results for apparent velocity (v_A^{Sg}=4.52 km/s) and backazimuth (103.5°) are still within the expected uncertainties.

4.3. *Beamforming of industrial-noise signals*

The seismic recordings were occasionally disturbed by coherent stationary 3 Hz signals with considerable amplitudes and duration of several minutes. As shown in fig. 12, the *f-k* analysis of the 2-4 Hz bandpass filtered signals revealed the maximum for a low apparent velocity of v_{app}= 1.3 km/s and a backazimuth of 31.7° with a relative power = 0.47. A probable explanation for this apparent velocity, which is typical for *Rg* phases, is a generation of the signals by a refuse dump located N of the town of CDC. In agreement with the low apparent

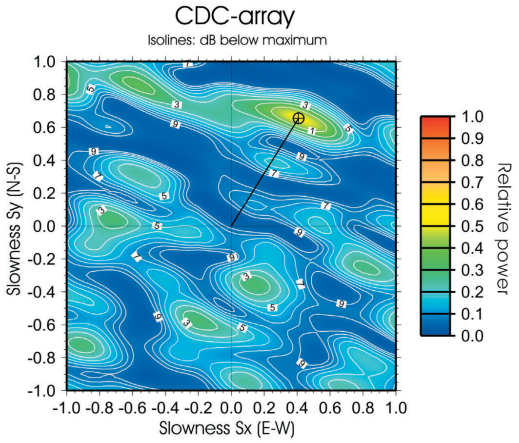

Fig. 12. *F-k* analysis of the coherent «3 Hz noise-signal», using nine vertical traces, bandpass filtered between 2-4 Hz. For the maximum peak level (relative power=0.47) a low apparent velocity of v_{app}=1.3 km/s was found, reaching the array from a back-azimuth of 31.7°.

Table I. Listing of observed *SNR*'s measured at a single site of the CDC array and on the CDC beam for different events. For more details see text.

Event	Δ	M_L	SNR_{SS}	M_{TSS}	SNR_{beam}	M_{Tbeam}	δM_T
1	120 km	2.5	8	2.1	48	1.3	0.8
2	40 km	2.0	10.5	1.45	38	0.9	0.55
3	30 km	1.8	12	1.2	30	0.8	0.4

velocity of the analysed phase (v_{app}= 1.3 km/s) the secondary maxima in the *f-k* plot of fig. 12 are due to spatial aliasing caused by the too large inter-station distances of the CDC-array.

5. Estimation of the magnitude threshold lowering due to the array

As introduced above, the CDC-test array data acquisition operated in a trigger mode. That means that the detection threshold was simply and solely determined by the STA/LTA trigger setting at the single array sites. On the other hand, uninterrupted data recording allows a detection algorithm to run continuously on the beam traces. In this case a much larger number of smaller events are detected, showing even more clearly the merits of an array installation.

Therefore, we can only extrapolate a lowering of the magnitude threshold on the basis of the *SNR* improvement reached by array beamforming after single site detection. The magnitude threshold M_T can be determined by subtracting from the event magnitude M_L a correction term M_C, which is defined as the ratio of the onsets SNR_{sig} and the *SNR* set as trigger threshold SNR_{tl}

$$M_T = M_L - M_C = M_L - \log\left[\frac{SNR_{sig}}{SNR_{tl}}\right]. \qquad (5.1)$$

Let us assume that the trigger level (tl) of the automatic detection process is preset to an SNR_{tl}= = 3, and that the signal of an event with M_L= 2.5 was recorded in a distance Δ with a SNR_{sig}= 21, then the magnitude threshold for an event occurring at this distance is M_T= 2.5 − log(21/3)= = 1.65. That means each event with a magnitude of 1.65 or larger should be detectable with this recording system and assuming identical noise conditions. The application of formula (5.1) to some events recorded by the CDC-test array is summarised in table I. The table lists the observed signal *SNR*'s once for the single stations (SNR_{SS}) and once for the beam (SNR_{beam}) and solved eq. (5.1) to get the corresponding magnitude thresholds M_{TSS} and M_{Tbeam} respectively. The lowering of the magnitude threshold δM_T is then just the difference between the two magnitude thresholds. For the CDC test array we found values of 0.4-0.8 magnitude units.

6. Conclusions and outlook

The purpose of the present feasibility study was to examine the merits of a small aperture array installation to improve of the detection and location of seismic events. This task is particularly interesting for the Tuscany Region, because of the low station density of the present installed network. One of the main advantages of a seismic array is its capability to monitor the seismicity in a relatively large area

with a low number of sensors – a scientific goal that normally can only be reached by a network consisting of distinctively more seismic stations.

F-k analysis of local and regional events, recorded by a nine element test array in the Upper Tiber Valley, showed for *Pg*/*Pn*-phases typical apparent velocities of $v_{app}^{Pg} = 5\text{-}6$ km/s and $v_{app}^{Pn} = 9\text{-}10$ km/s respectively. Particular care needs to be taken in the analysis of direct waves, which come from local events occurring just beneath the array. Keeping this in mind, a future array installation will need systematic calibration work.

Application of *f-k* analysis and beamforming on *S*-waves provided encouraging results. The advantage of using the horizontal components for wavenumber analysis of the *S*-phase leads to larger *SNR*, hence to more reliable *f-k* analyses results (*i.e.* larger signal coherence).

Due to the *SNR* improvement on the array beam trace, the detection threshold for local events could be lowered by $0.4 < M_L < 0.8$ with respect to a single station installation in the same area.

Acknowledgements

We thank Marco Cattaneo and the task force team for their help during the field work. Important suggestions during data analysis have been given by T. Kværna, J. Fyen, S. Mykkeltveit, and H. Bungum. We are grateful to S. Monna and two anonymous reviewers for their helpful comments. The field experiment was financed by the Gruppo Nazionale per la Difesa dai Terremoti (GNDT 01-555). Data analysis was performed at NORSAR during a research visit of T.B. at NORSAR, which was financed by the European Commission Programme «Access to Research Infrastructure» (contract no. HPRI-CT-2002-00189). NORSAR contribution no. 854.

REFERENCES

Braun, T. and J. Schweitzer (2002): Results from a small scale array installation in Central Italy and its merits for the local event detection processing capability, in *European Seismological Commission, ESC XXVIII Gen. Ass.*, Genova 2002, *Geophys. Res. Abstr.*, SCA/B-3.

Capon, J. (1969): High-resolution frequency-wavenumber spectrum analysis, *Proc. IEEE*, **57**, 1408-1418.

Cattaneo, M., P. Augliera and M. Demartin (2002): Seismic noise measurements for the Italian national seismic network, in *European Seismological Commission, ESC XXVIII Gen. Ass.*, Genova 2002, *Geophys. Res. Abstr.*, SCA/B-3.

Cocco, M. (2001): Development and comparison between methodologies for the evaluation of seismic hazard in seismogenic areas: application to the Central and Southern Apennines, *Report of GNDT Project 2000*.

Harjes, H.-P. (1990). Design and siting of a new regional seismic array in Central Europe, *Bull. Seismol. Soc. Am.,* **80**, 1801-1817.

Harjes, H.-P. and M. Henger (1973): Array-seismologie, *Z. Geophys.*, **39**, 865-905.

Kværna, T. (1989). On exploitation of small-aperture NORESS type arrays for enhanced *P*-wave detectability, *Bull. Seismol. Soc. Am.*, **79**, 888-900.

Kværna, T. and D.J. Dornboos (1986): An integrated approach to slowness analysis with arrays and three-component stations, in *NORSAR Semiannual Technical Summary*, 1 October 1985-31 March 1986, Kjeller, Norway, *Scientific Report 2-85/86*, 60-69.

Mykkeltveit, S. and H. Bungum (1984): Processing of regional seismic events using data from small-aperture arrays, *Bull. Seismol. Soc. Am.*, **74**, 2313-2333

Piccinini, D., M. Cattaneo, C. Chiarabba, L. Chiaraluce, M. De Martin, M. Di Bona, M. Moretti, G. Selvaggi, P. Augliera, D. Spallarossa, G. Ferretti, A. Michelini, A. Govoni, P. Di Bartolomeo, M. Romanelli and J. Fabbri (2003): A microseismic study in a low seismicity area of Italy: the Città di Castello 2000-2001 experiment, *Ann. Geophys.,* **46** (6), 1315-1324.

Schweitzer, J. (2001a): hyposat – An enhanced routine to locate seismic events, *Pure Appl. Geophys.*, **158**, 277-289.

Schweitzer, J. (2001b): Slowness corrections – One way to improve IDC products, *Pure Appl. Geophys.*, **158**, 375-396.

Schweitzer, J., J. Fyen, S. Mykkeltveit and T. Kværna (2002): Seismic Arrays, in *IASPEI: New Manual of Seismological Observatory Practice (NMSOP)*, edited by P. Bormann (Geoforschungszentrum Potsdam), vol. 1, ch. 9, pp. 52.

(received September 12, 2003;
accepted March 1, 2004)